Finding the stable structures of W_xN_{1-x} with an *ab-initio* high-throughput approach

Michael J. Mehl*
Center for Computational Materials Science, Naval Research Laboratory, Washington DC 20375

Daniel Finkenstadt and Christian Dane
Department of Physics, U.S. Naval Academy, Annapolis MD 21402

Gus L. W. Hart
Department of Physics and Astronomy, Brigham Young University, Provo, UT 84602

Stefano Curtarolo†
Materials Science, Electrical Engineering, Physics and Chemistry, Duke University, Durham NC 27708

(Dated: February 18, 2022)

Using density functional theory calculations, many researchers have predicted that various tungsten-nitride compounds $WN_x (x > 1)$ will be "ultra-incompressible" or "superhard", *i.e.* as hard as or harder than diamond. These compounds are predicted to have large bulk and shear moduli, (> 200 GPa) and to be elastically and vibrationally stable.

Compounds with such desirable properties must be energetically stable against decomposition into other compounds. This stability can only be found after the determination of the convex hull for W_xN_{1-x} lines which connect the lowest enthalpy structures as a function of composition. The phase diagram of the W-N structure is uncertain, both experimentally and computationally. Complex van der Waals forces play a significant role in determining the structure of solid N_2.

Here we use high-throughput calculations to map out the convex hull and other low energy structures for the W-N system. We find that the ground state of the system is the NbO structure, and that the WN_2 structures found by Wang *et al.* are also stable when van der Waals forces are neglected. Other proposed structures are above the convex hull of the W-N system. We show how the choice of density functional influences the shape of the curve and the structures that form the hull. In nitrogen-rich compounds, the choice of functional can dramatically change the structural parameters and mechanical behavior. Using any of the functionals, the bulk and shear moduli of the NbO phase are comparable to the WN_x compounds that have been claimed to be ultra-incompressible or superhard.

PACS numbers: 64.30.Ef, 64.70.kd, 61.50.Ah

arXiv:1403.2762v1 [cond-mat.mtrl-sci] 11 Mar 2014

INTRODUCTION

The search for materials with hardness comparable to diamond has centered on compounds with highly directional, short, and strong bonds.[1] In addition to diamond, these include other proposed carbon structures,[2, 3] cubic boron nitride[4], carbonitrides,[5] and transition metal borides.[6, 7] Over the past several years there has been considerable theoretical interest in tungsten nitride systems.[8–11] These computational studies predict that some compounds WN_x with $x \geq 2$ have large bulk and shear moduli. In one case[11] the hardness of the material was estimated to be on the same order as boro- and carbo-nitrides.

The present studies all address the issue of stability for various predicted WN_x compounds. This is done by showing they are elastically and/or vibrationally stable. It is also ensured the formation enthalpy of the compound is lower than the formation energy of its components, bcc tungsten, and αN_2.[12] That is,

$$\Delta H(W_xN_y) = [E(W_xN_y) - x\,E(W) - (y/2)\,E(\alpha N_2)]/(x+y)\ . \quad (1)$$

where $\Delta H(W_xN_y)$ is the formation energy per atom of a compound with stoichiometry W_xN_y, $E(W_xN_y)$ is the energy/formula unit of the compound, $E(W)$ is the equilibrium energy per atom of body-centered cubic tungsten, and $E(\alpha N_2)$ is the equilibrium energy per molecule of solid αN_2.

Condition (1) is necessary, but not sufficient, for structural stability. To be truly stable, a structure must lie on the convex hull constructed from the plot of enthalpy/atom versus composition for all possible phases

of the system. As we shall see, most of the WN_x structures referred to above do not fulfill this criterion.

The construction of the convex hull for the tungsten nitride system is non-trivial. The experimental phase diagram is not well defined.[13] Various papers have presented experimental results for cubic[14–17] ("β", composition 33-50% Nitrogen), hexagonal ("δ", composition 33-67% Nitrogen)[16], and tungsten-carbide (WC)[18] structures. Many of these are only found in thin films. There is no clear preference for a ground state structure at any composition. As a result, there is little guidance for computational first-principles studies of W-N. The computations that do exist start from a wide variety of structures.

Using an evolutionary technique, Wang *et al.*,[9] found that the lowest energy structure of WN_2 is hexagonal. The compound has either an hP3 structure, with space group $P\bar{6}m2$, or an hP6 structure with space group $P6_3/mmc$. At other stoichiometries the calculations are less certain. Previous papers have considered the ground state of WN to be NaCl,[19], tungsten carbide (WC),[8, 10] or NiAs.[20] More recently, Song *et al.* [10] looked at WN_3 in the P_3Tc structure, while Aydin *et al.*[11] have suggested that WN_4 has the ReP_4 structure.

None of these calculations addressed the complete range of stoichiometries in the WN system. What is needed is a method which quickly examines a wide variety of possible structures over large ranges of composition. One such method is AFLOW,[21] a high-throughput front end for electronic structure calculations.[22] AFLOW allows us to quickly examine a selected range of structures using high-performance supercomputers and modern density functional electronic structure techniques. The AFLOW prototypes' database, which was originally used to describe intermetallic alloys, [23–27] can easily be enlarged.[28] We were therefore able to include ionic and covalent structures which seem chemically similar to W-N. These include borides, carbides, oxides, and other nitrides.

In this paper we examine the possible ground states of the W-N system over a wide range of stoichiometries. Using the power of AFLOW, we can examine hundreds of possible W_xN_y structures. We show that the true ground state of W-N is related to what is known as βWN, and show why it exists over a wide range of stoichiometries. In addition, the bulk and shear moduli found for βWN are comparable to those WN_x compounds predicted to be ultra-incompressible[9] or superhard.[11]

The paper is organized as follows: Section describes the computational methods used. Section describes the main calculations of this paper: the determination of the convex hull for WN as a function of enthalpy (1). The majority of the calculations are done using the Perdew-Burke-Ernzerhof (PBE)[29] implementation of a Generalized Gradient Approximation density functional.

The ground state αN_2 structure of Nitrogen is influenced by van der Waals forces. We investigate these non-covalent forces using different density functionals in Section . In particular, the Local Density Approximation (LDA) [30, 31] calculations are presented in Section , and the so-called DF2 van der Waals functional (vdW-DF2)[32] is discussed in Section .

We then discuss several specific structures: Section we examine the cubic βWN phase, and the competing δWN phase in Section .[16] Section looks at the WN_2 structures found by Wang *et al.*,[9] along with other low energy WN_2 structures.

Section studies possible WN_3 structures, including the P_3Tc structure proposed by Song *et al.*,[10]. Section looks at the ReP_4 structure of WN_4 predicted by Aydin and coworkers.

We conclude with Section , which summarizes the results, and discuss the effects of the choice of density functional on the predictions for this system.

Finally, as a complete reconstruction of a the unit cell is necessary for the reproduction of any calculation, we list the crystallographic information for the most important structures discussed in this paper in the supplementary material.

METHODS

We began our search for the convex hull of the W-N system by using AFLOW [21, 22, 33] to quickly and efficiently search through a large database of structures. As the original AFLOW prototypes' database was for binary metallic alloys, [23–27] we extended it to include over fifty new structures. These include nitrides, oxides, borides, and carbides. The important structures, including all of those discussed in this paper, are described in the supplementary material.

Electronic structure calculations were done using the Vienna *Ab initio* Simulation Package (VASP),[34–36] including core state effects via the VASP implementation[37] of the Projector Augmented-Wave (PAW) method.[38] Since some our results were unexpected, we checked them against computations performed with ELK, an all-electron full-potential Linearized Augmented Plane Wave (FP-LAPW) code.[39]

AFLOW's default is to use the Perdew-Burke-Ernzerhof (PBE) implementation[29] of the Generalized Gradient Approximation (GGA) to Density Functional Theory (DFT).[40, 41] There are, however, substantial differences between PBE results and those from the Local Density Approximation (LDA).[30, 31] This was shown by Wang *et al.*[9], and we shall see further examples below. Accordingly, we have done some calculations using the LDA implemented in VASP, as shown in Section .

Molecular nitrogen, αN_2, is a van der Waals solid,[42] and neither the LDA nor the PBE-GGA correctly predict its lattice constant. We studied the effect of van der

Waals forces by utilizing the VASP implementation[43, 44] of the vdW-DF2 functional.[32] This functional was developed to handle the van der Waals interaction in general geometries, so we apply it over the entire range of compositions. These results are discussed in Section .

We used the VASP-supplied LDA and PBE PAW potentials for Nitrogen and Tungsten (specifically, May 2000 LDA and April 2002 PBE PAW potentials for N, and the July 1998 LDA and September 2000 Tungsten W_pv PAWs) from the VASP distribution. All calculations use a kinetic energy cutoff of 560 eV, which is 40% larger than the suggested cutoff for Nitrogen (400 eV). Unless otherwise stated, we let the AFLOW package determine the k-point mesh for each structure. This is usually set to use approximately the same density of k-points in reciprocal space for all structures.

For the NaCl structure, *e.g*, a $15 \times 15 \times 15$ Monkhorst-Pack grid[45] was originally used. For Wang *et al.*'s $P\bar{6}m2$ WN_2 structure we used a $15 \times 15 \times 9$ mesh. In the initial VASP calculations performed via AFLOW all structures are considered to be spin-polarized. However, in every structure the self-consistent magnetic moment was negligible, and the final calculations were all done assuming no moment.

The MedeA software system[46] was used to drive VASP in calculations of the phonon spectra and some other calculations. Elastic constants were computed by taking finite strains[47, 48] and determining the slope of the corresponding stress-strain curve (as implemented in the MedeA package, or using the native VASP option). Phonon frequencies were determined via the frozen-phonon approximation using the MedeA package.

THE GROUND STATE HULL AND LOW-LYING STATES OF TUNGSTEN NITRIDE

Overall we considered 350 possible structures from the expanded AFLOW prototypes' database. The equilibrium configurations for the important structures are described in the supplementary material. Fig. 1 shows the formation enthalpy per atom compared to αN_2 and bcc-W, as defined in (1).

The other structures on the convex hull in Fig. 1 are the two WN_2 structures found by Wang *et al.*[9], and the NbO structure (Fig. 2), which will be considered further in Section . To our knowledge this structure has never been considered as a candidate structure for WN. Its existence is not a complete surprise: WN has the same number of valence electrons as NbO, and the Nb and W atoms have similar valence shells ($4d^4 5s$ for Nb, $5d^4 6s^2$ for W). The electron gained by replacing Nb with W is lost again as we replace O with N.

The NbO structure is a supercell of the NaCl structure, with ordered vacancies on both the Na and Cl sites. Many of the other low-lying structures shown in Fig. 1 can be constructed by removing atoms from a supercell of the parent structure. Starting with the NaCl (B1), cubic ZnS (B3), and NiAs ($B8_1$) structures, we constructed supercells of the original cell (as described below) and removed atoms from both sites in a systematic manner. These structures are color/shape coded in Fig. 1. In all three cases, some supercells with multiple vacancies had lower energy than the parent structure. The ground state NbO can be constructed by removing atoms from the parent NaCl compound (NbO), while the $P\bar{6}m2$ WN_2 structure can be derived from either the NiAs or the tungsten carbide structure.

Some structures which have been predicted to be stable actually have enthalpies far from the convex hull. In particular, NaCl is over 0.3 eV/atom above NbO, and the WC and NiAs structures are over 0.2 eV/atom above NbO. We will discuss the predicted P_3Tc structure for WN_3 and ReP_4 structure for WN_4 in later sections.

RESULTS USING DIFFERENT DENSITY FUNCTIONALS

As noted above, solid αN_2 is bound by the van der Waals interaction between molecules. Furthermore, Wang *et al.* found a substantial change in the enthalpy of their WN_2 systems when changing from PBE to LDA functionals. This suggests that the choice of functional may well change our predictions of the structure in the W-N system. We tested this by comparing results for selected structures using three different density functionals: the Perdew-Burke-Ernzerhof Generalized Gradient Expansion (PBE),[29] the Local Density Approximation (LDA),[30, 31] and the van der Waals functional developed by Dion *et al.* (vdWDF2),[32] as implemented in VASP by Klimeš *et al.*[43, 44] We began our tests by considering the known ground states of the end-points, αN_2 and bcc-W.

First consider nitrogen. There is a computational problem in using VASP to compute the equilibrium lattice constant for all of the nitrogen structures considered here. The bulk modulus of the molecular N_2 crystal in any phase is extremely small, about 1 GPa.[49] As a result, algorithms which stop searching for a minimum when the pressure reaches some small number will fail here unless an extremely small tolerance is used. In addition, while the calculation of the total energy of a system is variational, that of the pressure is not. As a result, the pressure calculation will not converge unless we use a much larger plane-wave basis set. We eliminated this problem for the N_2 phases by explicitly calculating $E(V)$ at discrete points, bounding the minimum, and using a fourth-order Birch fit[50] to determine the equilibrium lattice constant.

Experiments have determined that αN_2 is cubic with either space group $P2_13$-T^4 (#195), which has no in-

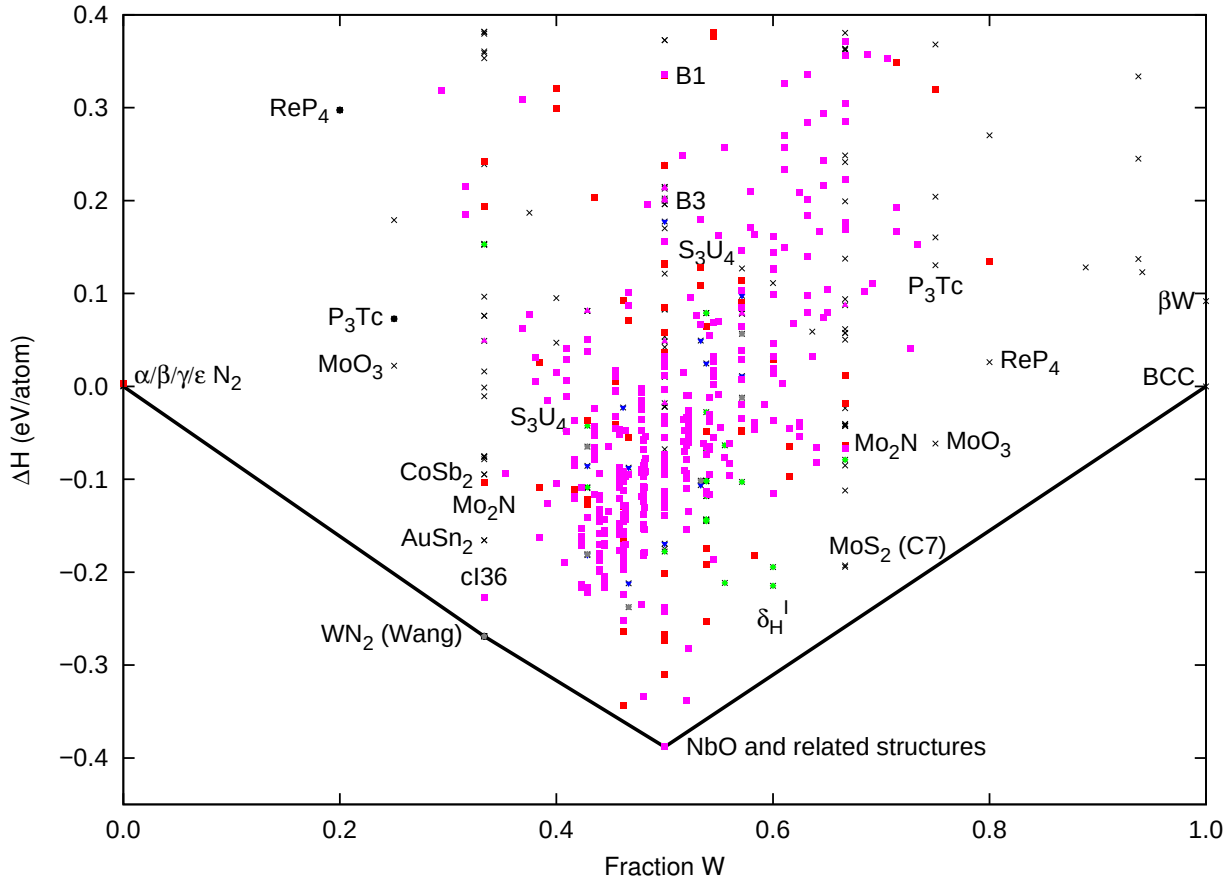


FIG. 1: (Color online) Low-enthalpy structures of Tungsten Nitride, calculated using PBE. Each cross gives the enthalpy of a structure from the AFLOW database, as described in the supplementary materials. The solid colored symbols denote structures constructed by removing atoms from a base structure and allowing the system to relax, as described in the text and the supplementary material. Red squares: NaCl and constructed by removing atoms from supercells of NaCl, including possible β-phase structures.[14] Green diamonds: the δ-phase and related structures.[16] Upward pointing purple triangles: Cubic ZnS (B3) and related structures. Downward pointing blue triangles: NiAs ($B8_1$). Gray pentagons: WC and related structures. The black circles indicate structures which other researchers have described as hard.[9, 11] Note that Wang *et al.*'s $P\bar{6}m2$ WN_2 structure could be grouped with the NiAs structures as well as the WC structure.

version site, or $Pa\bar{3}$-T_h^6 (#205), which contains an inversion.[12] In VASP the energy and structural differences between the two structures is negligible. In fact, the energy difference between the five N_2 structures shown in Fig. 1 is less than 4 meV/atom. This being the case, here we present only the results for the highest symmetry structure, $Pa\bar{3}$. The results for the equilibrium geometry of this phase for all three functionals are given in Table I.

The PBE GGA overestimates the equilibrium lattice constant of αN_2 by 9% while the LDA underestimates it by almost 8%, as was also found by Mailhoit *et al.*.[52] Both of these errors are much larger than found for most elements.[53] If we consider the van der Waals interaction using the vdW-DF2 functional, we get an error in the lattice constant of 5.2%, which, while not ideal, is a substantial improvement on both the LDA and PBE results. All of the calculations give essentially the same distance for the N-N bond, suggesting that errors in the calculations are due to the long-range interaction between the molecules. Both LDA and vdW-DF2 substantially over-

TABLE I: Equilibrium lattice constant, internal parameter, and equilibrium bulk modulus for the $Pa\bar{3}$ structure of αN_2, as determined using various density functionals and compared to experiment.[12, 49] The lattice is simple cubic, and the nitrogen atoms sit on the (8c) Wyckoff position, which has one internal parameter, x. The equilibrium lattice constant and bulk modulus are determined from a fourth order Birch fit. The quantity d(N-N) is the length of the nitrogen-nitrogen bond in N_2 molecules.

Functional	PBE	LDA	vdW	Exp[12]
a (Å)	6.187	5.223	5.511	5.659
x	0.052	0.061	0.058	0.056
d(N-N) (Å)	1.11	1.10	1.11	1.10
K_0 (GPa)	0.788	5.70	4.69	1.2[49]

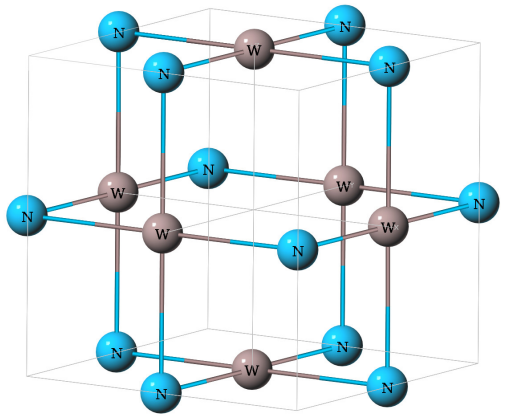


FIG. 2: (Color Online) WN in the NbO structure, constructed by taking equally spaced vacancies from both sites of the NaCl structure. The PBE functional predicts the equilibrium lattice constant to be 4.131Å.

TABLE II: Equilibrium lattice constant and bulk modulus for bcc tungsten, as determined using various density functionals and compared to experiment.[12, 51] The equilibrium lattice constant and bulk modulus are computed from a fourth order Birch fit to energy versus volume data.

Functional	PBE	LDA	vdW	Exp
a (Å)	3.190	3.143	3.250	3.165[12]
K_0 (GPa)	304	337	267	323[51]

estimate the bulk modulus, while PBE underestimates it by about 35%. The vdW-DF2 prediction demonstrates the importance of van der Waals interactions in Nitrogen systems.

Similar calculations were carried out for the ground state body-centered cubic structure of tungsten. The results are presented in Table II. In this case the equilibrium lattice constant determined by VASP is almost exactly identical to the result from a Birch fit to energy-volume data. We use the latter so that we can also compute the equilibrium bulk modulus and compare it to experiment.[51] All three functionals produce reasonable values for the equilibrium lattice constant and bulk modulus, with the LDA yielding perhaps the best agreement.

The conclusion of this brief study is that none of the three functionals is ideal for describing both tungsten and nitrogen structures. All three do give the same ordering of the low-energy states at both endpoints. As we shall see below, this agreement does not extend to W_xN_{1-x} compounds, and the choice of functional significantly affects the predicted shape and structural composition of the convex hull.

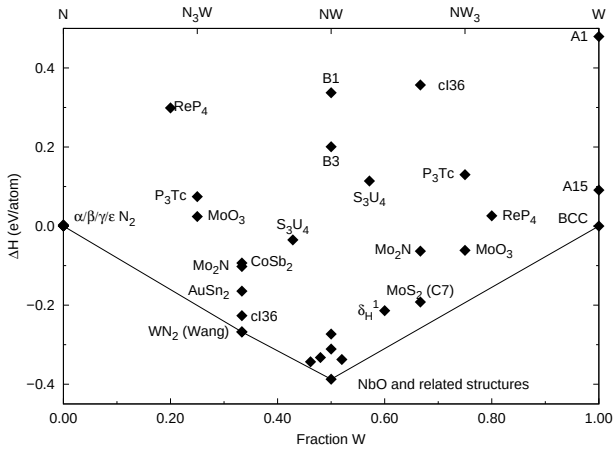


FIG. 3: The relative enthalpy (1) of structures making up the ground state hull. and other selected structures for the Tungsten Nitride system. These were calculated using the Perdew-Burke-Ernzerhof (PBE) functional[29] with VASP. The state labeled cI36 at x = 1/3 is the NbO structure with additional defects, as described in Section .

LDA results

The calculations leading to the results in Table I show that the PBE functional improperly describes the ground state structure of αN_2. This calls into question the predicted shape of the ground state hull shown in Fig. 1. We examine the possible errors in the PBE by redoing a subset of our calculations with other density functionals. We have selected a data-set of 34 structures, including end points, low-lying states (WN_2, NbO and related structures, *etc.*), "interesting" states (P_3Tc, ReP_4), and "parent" structures (NaCl, B3-ZnS). All these are described in the supplementary material. The resulting enthalpy calculation is shown in Fig. 3 for the PBE functional, and Fig. 4 for LDA.

The composition of the hull is unchanged when going from PBE to LDA. Its shape changes visibly, as the hexagonal WN_2 phases are now competitive with the NbO phase. Within the LDA, all structures are more tightly bound compared to the endpoints, by a factor of two or more. On the tungsten right side of the LDA plot two structures, δ_H^I (discussed in Section) and MoS_2, are extremely close to the tie-line between the NbO structure and bcc tungsten. This indicates that the LDA functional may well be the best choice for calculations on the tungsten-rich side, since several of δ phases are observed experimentally.[16]

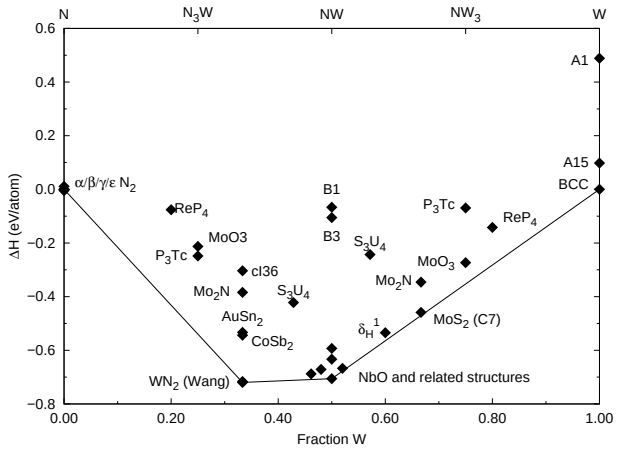


FIG. 4: The relative enthalpy (1) of structures making up the ground state hull, and other other structures for the Tungsten Nitride system. These were calculated using the Local Density Approximation (LDA) with VASP. The state labeled cI36 at x = 1/3 is the NbO structure with additional defects, as described in Section .

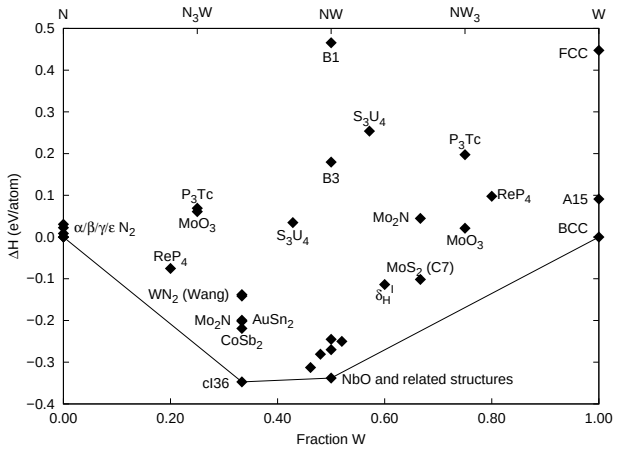


FIG. 5: The relative enthalpy (1) of structures making up the ground state hull and selected other structures for the Tungsten Nitride system. These were calculated using vdW-DF2 van der Waals functional with VASP. The state labeled cI36 at x = 1/3 is the NbO structure with additional defects, as described in the Section .

van der Waals results

At first glance, Fig. 5, which shows the vdW-DFT convex hull for W_xN_{1-x}, looks similar to the PBE (Fig. 1) and LDA (Fig. 4) diagrams. On closer examination we see substantial differences. The principle difference is that the vertex of the hull at x = 1/3 is not one of the WN_2 structures found by Wang *et al.*. Rather, it is a cubic structure we have labeled cI36. In fact, the Wang structures are above a line drawn from αN_2 and NbO, and so would not be on the hull even if the cI36 structure was not present. The ReP_4 structure is now rather low in energy, about 0.1 eV/atom away from the tie line. We will examine these structures in more detail in later sections.

CUBIC (β) WN STRUCTURES

Hägg[14, 18] identified the β phase in the WN system as cubic, with the approximate composition W_2N. The tungsten atoms form a face-centered cubic lattice and the nitrogen atoms are randomly distributed, presumably at the octahedral sites.[16] Chiu and Chuang[54] grew thin films of nominal composition WN using metallo-organic chemical vapor deposition (MOCVD). They found a cubic structure of composition WN_x, with $0.7 < x < 1.8$. Where the composition is near W_2N they found a lattice constant of 4.125Å, rising to 4.154Å at stoichiometry and to 4.172Å as x approaches 1.8. They state that the tungsten atoms remain on FCC sites. For $x = 1$ the nitrogen atoms fill the octahedral sites. For $x < 1$ there are vacancies on the octahedral sites, and for $x > 1$ nitrogens populate both the octahedral and tetrahedral sites.

Computationally, we find something different, as seen in Figures 3-5. All three functionals predict NbO to be the ground state structure. NbO has space group $Pm\overline{3}m$ (#221). The tungsten atoms are on the (3c) Wyckoff sites, and the nitrogen atoms are on the (3d) sites (or *visa versa*). It can be described as an eight-site supercell of the sodium chloride structure with ordered vacancies on both the Na and Cl sites, as shown in Fig. 2. Within the PBE-GGA, we find the equilibrium lattice constant to be 4.131Å.

This is in reasonable agreement with the experimental value of 4.125Å found by Chiu and Chaung[54] and reported in the Alloy Phase Diagrams.[13] Chiu and Chaung describe the site as having all FCC and octahedral sites filled, *i.e.* the NaCl (B1) structure. Instead we find vacancies on both sites. The minimization of the actual B1 structure gives a lattice constant of 4.366Å, in close agreement with other calculations.[8, 19] This suggests that what Chiu and Chaung were seeing was actually the NbO structure, or something very close to it.

Table III lists the structural and elastic parameters of WN in the NbO structure using all three functionals. The structure is elastically stable, with all of the Born criteria[55] satisfied. We also estimate the shear modulus using the average of the Hashin-Shtrikman bounds.[56, 57] The bulk and shear moduli are comparable to those found by Wang *et al.* for the predicted hexagonal WN_2 structures, the WN_3 structure studied by Song *et al.*,[10] and the WN_4 structure predicted by Aydin *et al.*[11] We have not tried to predict the actual hardness of the material, but the cubic NbO structure of WN is certainly difficult to compress.

We also checked the vibrational stability of the NbO

TABLE III: Equilibrium lattice and elastic constants of WN in the NbO structure, (Space Group $Pm\bar{3}m$ #221, Wyckoff positions (3c) and (3d)). These were computed by VASP using the appropriate PAW potentials for each exchange-correlation functional. Elastic constants (in GPa) were computed by finite strain calculations.[47, 48] The isotropic shear modulus G is the average of the Hashin-Shtrikman bounds for a cubic system.[56, 57]

Functional	a (Å)	C_{11}	C_{12}	C_{44}	B	G
LDA	4.078	884	140	177	388	239
PBE	4.131	754	126	173	335	220
vdW-DF2	4.208	655	120	154	298	192

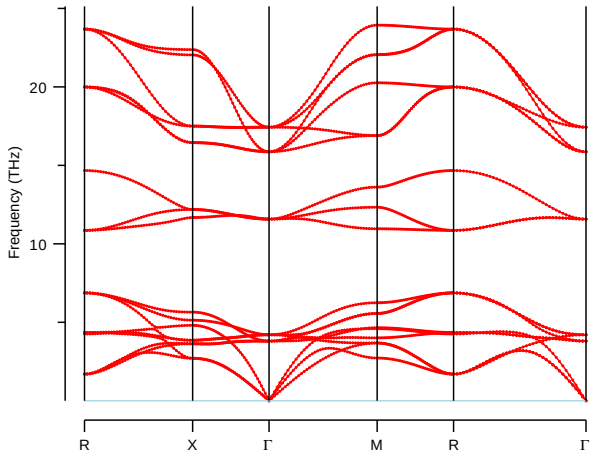


FIG. 6: (Color Online) Phonon frequencies along high-symmetry lines for the NbO structure of WN, found via the MedeA package.[46] No imaginary phonon frequencies were found, indicating that this structure is stable against small amplitude vibrations.

structure by computing the phonons along high symmetry lines using the MedeA software package.[46] The results for the PBE calculation are shown in Fig. 6. We found no imaginary frequencies over the entire Brillouin zone, leading us to the conclusion that the NbO structure of WN is at least metastable. Since this is the lowest energy structure found, we believe that this is the stable ground state structure of WN at this composition.

The electronic band structure and density of states of the NbO structure of WN are given in Figures 7 and 8, respectively. The structure is metallic, with the tungsten d bands dominating the region near and above the Fermi level.

The prediction of the hitherto unseen NbO ground state was unexpected (albeit perhaps unsurprising in retrospect), and could possibly be an artifact of either the PAW potentials or the PBE exchange-correlation approximation. Accordingly, we compared the energy of the NbO phase of WN to several of the usual suspects for the WN composition. We used two techniques:

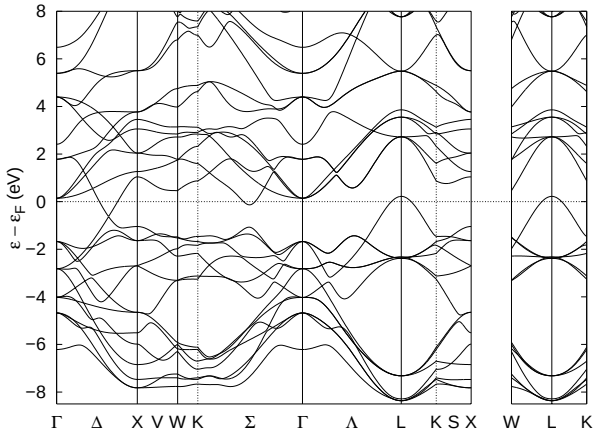


FIG. 7: The electronic band structure of WN in the NbO structure at the PBE equilibrium (a = 4.131 Å).

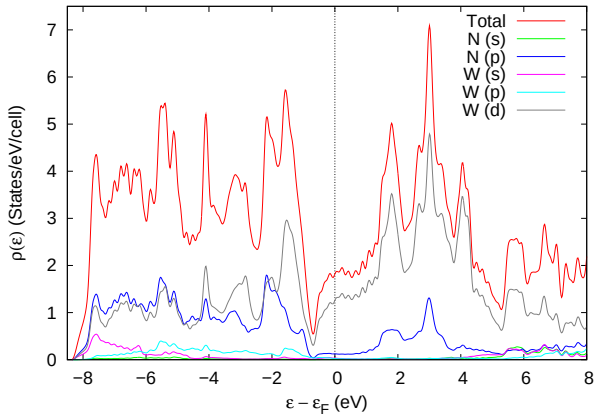


FIG. 8: (Color Online) The electronic density of states and angular-momentum decomposed density of states for WN in the NbO structure. These were computed via the tetrahedron method in VASP. The primary contributions are from the N-p and W-d states, with the W-d states dominating the conduction band.

1. All electron calculations using the Elk FP-LAPW code[39] within the PBE GGA. Elk does not easily do structural relaxation, so we used the equilibrium structural parameters from the VASP PBE GGA calculations and the same k-point mesh. We used the supplied muffin-tin files for W and N, and set the energy cutoff using a value of $RG_{max} = 9.0$.

2. LDA[30, 31] calculations using the LDA PAW potentials supplied with VASP. In this case we allowed the structures to fully relax. All other parameters, including the energy cutoff, we kept the same as in the PBE GGA calculations.

Table IV shows the results. The energy differences between the VASP and Elk PBE calculations are all less than 0.02 eV/atom. The VASP LDA results show the

TABLE IV: Energy differences for various structures of WN with 50-50 stoichiometry, computed using VASP with PBE PAW, the Elk FP-LAPW code, and VASP with LDA PAW. The Elk calculations used the relaxed structures from the PBE PAW runs, while the VASP LDA calculations were fully relaxed. In each case the energy of the NbO structure was set to zero, and we show energy differences between the structures in eV/atom. In the $B8_1$ (NiAs) calculation the N atom was placed on the As (Wyckoff position 2c) site.

Structure	VASP PBE	Elk	VASP LDA
NbO	0	0	0
$B8_1$ (NiAs)	0.219	0.191	0.124
B_h (WC)	0.315	0.303	0.233
B1 (NaCl)	0.590	0.591	0.603
B3 (ZnS)	0.723	0.735	0.637

same ordering of the structures, although the energy differences are larger (as much as 0.1 eV/atom). We conclude that the NbO state is the lowest energy structure of all the 50-50 stoichiometries structures we have studied.

Since the NbO ground state WN can be considered as an NaCl structure with ordered defects, it is logical to ask if any other pattern of defects produce low energy structures. As mentioned at the beginning of this section, the literature[13, 14, 18, 54] suggests that βWN is Nitrogen deficient, with composition approximately $WN_{0.7}$. The simplest Nitrogen deficient structure we can make is to take one atom out of an 8 atom supercell of the NaCl structure, or, equivalently, add one Tungsten atom back into the NbO structure. Experimentally, the prototype for this structure is S_3U_4,[58] and so we will refer to it by that designation. As shown in Figs. 3-5, the enthalpy/atom of W_4N_3 is lower in the S_3U_4 structure than the enthalpy of WN in the NaCl structure, but it is still significantly larger than the enthalpy of WN in the NbO structure. As a test, we also studied Nitrogen-rich W_3N_4 in the S_3U_4 structure. We found that its enthalpy was also lower than NaCl – and even lower than W_4N_3 in the S_3U_4 structure – but still well above the enthalpy of the NbO structure.

We continued along this path by constructing vacancy patterns in NaCl supercells containing 8, 16, and 32 atoms. We considered a variety of possible unit cells where a given site in the supercell was "on" (occupied) or "off" (vacancy). We then fully relaxed the unit cell, and computed the enthalpy according to (1). For an N atom cell there are $2^N - 1$ possible combinations. For the larger cells we have therefore currently placed constraints on the search algorithm such that the composition is WN_x with $x \in [1/2, 3/2]$. All of these structures can be considered as candidates for Hägg's β phase.

For the 8 atom supercell (a simple cubic supercell of NaCl) we looked at all 255 combinations. We found 34 unique structures, including NbO itself, CsCl, S_3U_4, ReO_3,[59] cubic perovskite (with formula unit NW_4 or WN_4), monatomic fcc (*Strukturbericht* symbol A1), and simple cubic (A_h), as well as a variety of lower symmetry structures.

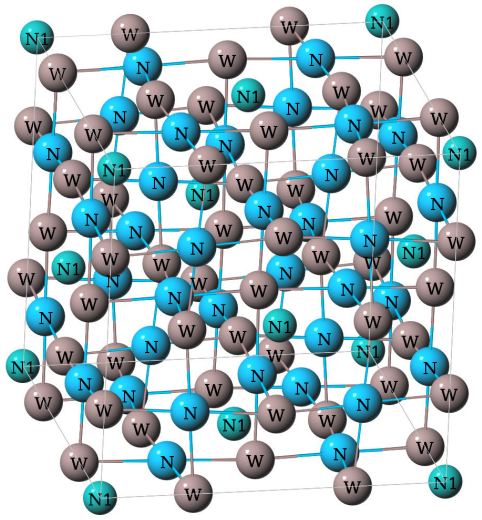


FIG. 9: (Color Online) The N_7W_6 supercell. The atoms labeled N and W form the NbO structure. The atom labeled N1 was added at one of the vacancy sites, maintaining cubic symmetry. Note the substantial relaxation of the W atoms away from the N1 atom. Aside from NbO this is the lowest enthalpy structure of all those studied.

The 16 atom supercell is face-centered cubic, with all primitive vectors doubled from the original NaCl cell. We looked at 26 structures with composition $W_{m+4}N_{n+4}$, where $m, n \geq 4$.

The 32 atom supercell of the NaCl structure is body-centered cubic. In this case we only looked at structures closely related to the NbO structure. Thus we examined $W_{13}N_{12}$, which has one of the vacant W sites in the NbO structure occupied, and $W_{12}N_{11}$, which has an extra N atom removed from the NbO supercell. We looked at 18 structures of varying composition. Aside from the near 50-50 stoichiometric structures, the most interesting one has the composition $N_{12}W_6$. This structure will be described in detail in Sec. .

The low enthalpy structures generated by this process are plotted as red squares in Fig. 1. All are closely related to NbO, either by the addition or subtraction of an additional N or W atom from the 16 or 32 atom supercells. For example, the lowest energy structure after NbO plotted on the graph has composition N_7W_6. We constructed this structure starting with the NbO structure expanded onto the 16 atom supercell. We then placed an additional N atom back onto one of the vacant sites, and allowed the system to relax. The cell is shown in Fig. 9. There is every reason to suspect that with increasing supercell size we can find a large number of structures with enthalpy close to NbO, with varying compositions.

Our calculations show that low-lying β structures must have vacancies on both the N and W sites. Since there are a large number of these structures very close to the NbO state, entropic effects must be large. The observed "sodium chloride" structure, with lattice constant 4.12-4.14Å,[13, 15] is most likely formed with approximately 25% vacancies on each site. These vacancies will no doubt be ordered locally, but when averaged over the entire crystal will look like the NaCl structure. The lattice constant of this phase will be closer to NbO (4.131Å) than pure NaCl (4.366Å). The experimentally observed lattice constant of 4.12-4.14Å is consistent with this conjecture.

THE HEXAGONAL δ_H STRUCTURES

Khitrova and Pinsker[16] detailed six hexagonal "δ_H" and rhombohedral "δ_R" phases in the W-N system, with compositions ranging from NW_2 (δ_H^{II}) to N_2W (δ_H^{III}). Four of these structures were found to have vacancies on one of the tungsten sites. Since we were primarily interested in the nitrogen-rich structures close to the convex hull we did not do exhaustive searches for ordered vacancies in these structures. We did, however, find that the δ_H^I structure, taken without defects and thus having composition N_2W_3, had the lowest energy of all the δ structures. Fig. 1 shows that this structure is within 0.1 eV/atom of the tie-line within the PBE, and the structure is barely above the tie-line within the LDA (Fig. 4). It is quite likely that searches for ordered defect structures in supercells of δ_H^I will show lower energies.

PREDICTED WN_2 STRUCTURES

In both the LDA and PBE the lowest lying states with composition WN_2 are the hexagonal structures found by Wang *et al.*[9]. Our structural parameters agree with theirs, as shown in the early columns of Table V. We also found the elastic constants of both structures, including the average of the Voigt[60] and Reuss[61] bounds on the isotropic bulk and shear moduli. These also agree with Ref. 9, confirming that these structures are candidates for superhard WN.

Both of these structures can be described as N_2 dimers separated by Tungsten planes. We might therefore expect the addition of van der Waals forces between the dimers to be significant. Structurally, as shown in the last column of Table V, there is little difference between the vdW-DF2 calculations and the LDA or PBE. The hexagonal unit cell is expanded slightly in both structures, as is the N_2 dimer separation, but the changes are not substantial. The energetic difference, is, however, quite large. In the LDA (Fig. 4) and PBE (Fig. 3) these WN_2 structures have enthalpies/atom comparable to the NbO structure of WN.

TABLE V: Equilibrium structural parameters for the hexagonal N_2W structures found by Wang *et al.*[9] The low symmetry hP3 structure is in space group $P\bar{6}m2$-D_{3h}^1 (#187), with nitrogen atoms at the (2g) Wyckoff positions ($00z$) and the tungsten atom on the (1d) site ($\frac{1}{3}\frac{2}{3}\frac{1}{2}$). In the high symmetry hP6 structure ($P6_3/mmc$-D_{6h}^4, #194) the nitrogen atoms are on (4e) sites ($00z$), and the tungsten atoms are on (2d) sites ($\frac{1}{3}\frac{2}{3}\frac{3}{4}$). For the LDA and PBE functionals we show our results (O), and the results of Wang *et al.* (W). R_{N-N} and R_{N-W} are the length of the respective bonds. The elastic constants are in GPa. The isotropic bulk (B) and shear (G) moduli are averages of the Voigt[60] and Reuss[61] bounds.

Functional	LDA		PBE		vdW-DF2
Low symmetry $P\bar{6}m2$, hP3					
	O	W	O	W	O
a (Å)	2.887	2.887	2.928	2.933	3.000
c (Å)	3.877	3.877	3.916	3.918	3.974
z	0.1804	0.1804	0.1813	0.1814	0.1824
R_{N-N} (Å)	1.399	1.399	1.421	1.421	1.450
R_{N-w} (Å)	2.077	2.077	2.104	2.104	2.143
C_{11}	638	654	573	588	493
C_{33}	1056	1082	954	973	827
C_{44}	241	260	222	232	191
C_{12}	207	213	183	191	159
C_{13}	230	248	193	206	157
B	396	412	351	255	297
G	246	255	226	231	195
High symmetry $P6_3/mmc$, hP6					
	O	W	O	W	O
a (Å)	2.893	2.893	2.934	2.939	3.007
c (Å)	7.714	7.714	7.790	7.796	7.891
z	0.0898	0.0898	0.0902	0.0902	0.0907
R_{N-N} (Å)	1.392	1.392	1.406	1.406	1.431
R_{N-w} (Å)	2.078	2.078	2.105	2.105	2.144
C_{11}	633	642	568	579	486
C_{33}	1051	1078	952	973	827
C_{44}	249	262	228	233	197
C_{12}	213	217	187	195	161
C_{13}	237	252	199	211	197
B	399	411	353	364	298
G	245	252	225	228	195

Adding van der Waals forces changes the shape and composition of the ground-state convex hull. The ground state structure of the system is now the body-centered cubic structure shown in Fig. 10. Although it is not obvious, this structure was constructed from a 32-atom body-centered cubic supercell of NaCl. This results in a structure with space group $Im\bar{3}m$-O_h^9, #299. Nitrogen atoms are at the (2a), (6b), and (24h) Wyckoff positions of the BCC lattice, while tungsten atoms are on the (8c), (12d), and (12e) sites. We remove the atoms on the (2a), (6b), (8c), and (12e) sites, leaving 12 N atoms

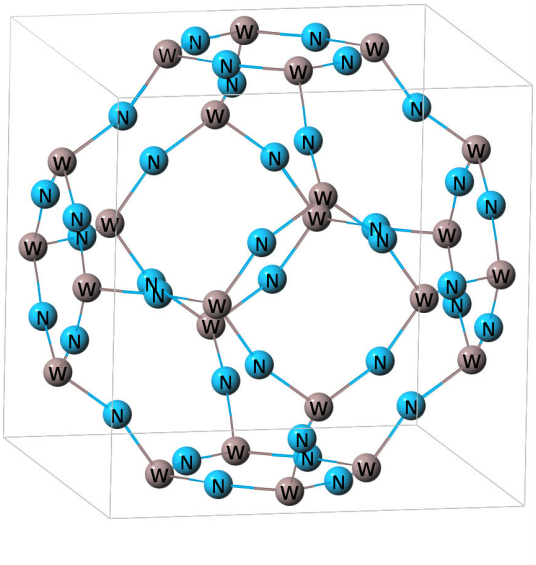


FIG. 10: (Color online) The cI36 structure predicted for N_2W. The basic structure looks the same using LDA, PBE, and vdW-DF2 functionals. The exact dimensions are described in Table VI. Note that this is a body-centered cubic lattice, so the center of the cube and the cube corners are equivalent sites.

TABLE VI: The cI36 structure of WN_2, constructed from a 32 atom body-centered cubic supercell of the NaCl structure. The space group is $Im\bar{3}m$-O_h^9 (#229), the nitrogen atoms occupy the (24h) Wyckoff positions ($0yy$), and the tungsten atoms occupy the (12d) sites ($0\frac{1}{4}\frac{1}{2}$). The first N-W-N angle is for atoms lying on the surface of the cube cell. The second case has one of the N atoms in the interior of the cube.

Functional	LDA	PBE	vdW
a (Å)	10.273	10.383	10.490
y	0.1454	0.1455	0.1455
W-N bond (Å)	1.840	1.860	1.879
Angles			
W-N-W	108.7°	108.6°	108.5 °
N-W-N (face)	108.7°	108.6°	108.5°
N-W-N (interior)	109.9°	109.9°	110.0°

at the $(0, y, y)(24h)$ Wyckoff positions, and 6 W atoms on Wyckoff sites $(01/41/2)(6d)$. The nitrogen atoms are then allowed to relax away from the $y = 1/4$ value of the original supercell. We have relaxed this structure, which we will designate by its Pearson symbol, cI36, using all three functionals. The results are shown in Table VI.

Within the LDA the cI36 structure is not particularly noteworthy. Its enthalpy is above the tie-line, well above that of our other WN_2 structures, including Mo_2N, another structure which can be formed by removing atoms from the NaCl structure. With the PBE functional the cI36 structure is less than 0.1 eV/atom above the ground

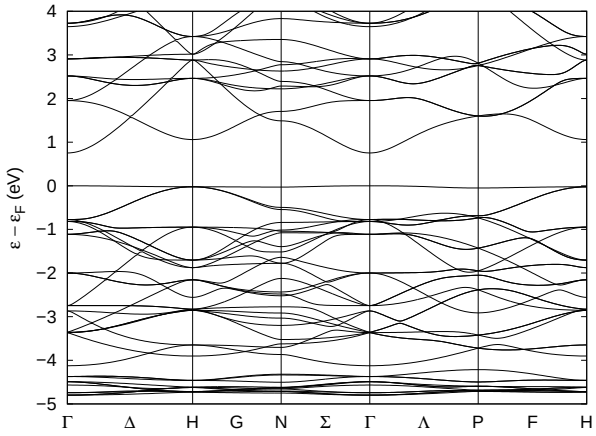


FIG. 11: The electronic band structure for the body-centered cubic cI36 structure of WN_2 described in the text. Calculations were done using the vdW-DF2 functional, including van der Waals forces, within VASP. The top valence band has a very small dispersion, dropping to -0.05 eV below the Fermi level at P. The gap is 0.75 eV, and is direct at Γ. The LDA and PBE calculations produce similar band structures.

state hull, below all of our test structures save for the two from Wang *et al.*

Finally, when we use the vdW-DF2 functional the cI36 structure becomes the lowest energy structure. This is not necessarily because the van der Waals interaction promotes this structure. Rather, as is seen in Fig. 5, the energy of the hexagonal WN_2 structures moves up compared to the αN_2 and bcc W endpoints, even though the lattice constants, atomic positions, and bond lengths are little changed. Since there is no experimental evidence for any of the WN_2 structures, and all three functionals are approximations with well-known limitations, we cannot determine which picture is correct.

The cI36 structure is an insulator. The electronic band structure, obtained using the vdW-DF2 functional, is shown in Fig. 11. The phase is also elastically stable, as is shown in Table VII. We computed the elastic constants using the finite-strain method,[47] fixing the primitive cell in its strained position while allowing the atoms to relax within the cell, as allowed by symmetry. Whereas cubic WN, in the NbO structure, is quite hard, the shear moduli of the cI36 structure is predicted to be very small by all functionals.

Further work on possible WN_2 phases was done by Song and Wang,[10] who studied WN_2 in the $CoSb_2$ structure.[62] As shown in Figs. 3-5, this structure is 0.1-0.2 eV above the hexagonal WN_2 structures for all three functionals. It is therefore never a candidate for the W-N ground state. We also found two other structures with energies close to the $CoSb_2$ structure: Mo_2N,[63] which is another structure constructed by removing atoms from a supercell of NaCl, and $AuSn_2$.[64] Neither structure is a candidate for the ground state of WN_2. Parameters of

TABLE VII: Elastic constants for the cI36 structure of WN_2, computed using the LDA, PBE, and vdW-DF2 functionals. Elastic constants were computed by the finite strain method,[47] allowing the atoms to relax at each strain while fixing the unit cell. Equilibrium structural parameters are taken from Table VI. B is the equilibrium bulk modulus, and all elastic constants are in GPa. The shear modulus G is an average of the Hashin-Shtrikman bounds.[56, 57]

Functional	C_{11}	C_{12}	C_{44}	B	C_{11} - C_{12}	G
LDA	119	77	13	91	42	15
PBE	112	72	13	85	41	16
vdW-DF2	104	65	12	78	39	14

the minimum energy structures for all of these phases are given in the supplementary material.

WN_3 STRUCTURES

Song and Wang[10] considered WN_3 in the P_3Tc structure,[65] and found that it has a negative enthalpy relative to αN_2 and bcc-W. They showed that the elastic constants met the Born criteria for long-wavelength stability,[55] and so claim that it is a possible state of WN_3. As seen in Fig. 4, within the LDA the P_3Tc does have negative enthalpy compared to the end points. However, it is over 0.2 eV/atom above the tie-line using the LDA, PBE, and vdW-DF2 functionals. This means that the PTc_3 structure cannot be an equilibrium state in the W-N system, although it is possible it may exist as a metastable state.

We also looked at a competing structure, Molybdite (MoO_3).[66] This structure has the same space group (*Pnma*) as P_3Tc and the same occupied Wyckoff positions. Yet when starting from different initial conditions it relaxes to a much different unit cell, even though the energy is comparable to the PTc_3 structure. The minimum-energy structures for both P_3Tc and MoO_3 are given in the supplementary material.

WN_4 STRUCTURE

The WN_4 structure proposed by Aydin *et al.*[11] is the most interesting candidate structure we studied. Using ReP_4 as its prototype,[67] within the LDA they predicted it to have relatively large bulk and shear moduli (338 and 198 GPa, respectively). In addition its hardness was estimated to be near that of some of the superhard borocarbides and carbonitrides.

We investigated this structure in some detail. We relaxed the structure provided by the authors of Ref. 11, using the LDA, PBE, and vdW-DF2 structures. Within the LDA we quickly found an equilibrium position close to the published result. When we next computed the

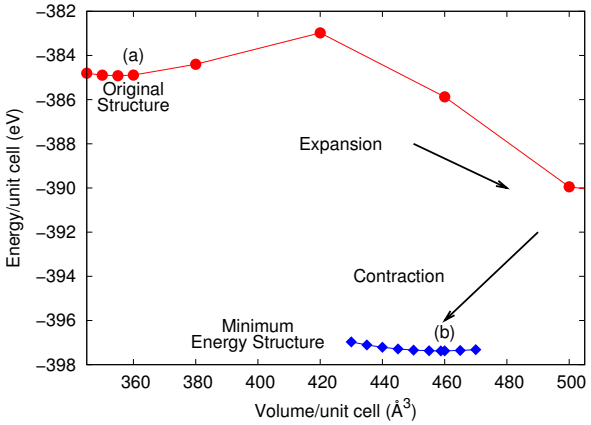


FIG. 12: (Color online) Energy versus volume calculations for WN_4 in the ReP_4 structure, using VASP and the LDA exchange-correlation functional. The original calculation in the upper left-hand corner found a structure close to that reported previously.[11] When the structure was expanded past a volume of 420 Å^3, the energy started to drop rapidly. Reversing the expansion caused another shift in the structure, where the energy finally reached the values shown near the bottom of the graph. The labels (a) and (b) correspond to the structure pictures in Fig. 13. All the calculations use the same space group, *Pbca*-D_{2h}^{15}(#61), and the N and W atoms remained on (8c) Wyckoff positions.

energy-versus volume curve, in order to determine the bulk modulus, we inadvertently expanded the structure past the unit cell volume of 420 Å^3. The structure quickly dropped in energy, as shown in Fig. 12. Compressing the lattice then caused a transformation to yet another configuration, labeled (b) in Fig. 12. Note that at no time did the structure leave the *Pbca* space group of ReP_4, and the atoms remained on (8c) Wyckoff sites. Most likely the finite jumps in volume we applied allowed for large relaxations in the atomic positions, causing a jump from one local minimum to another. It is possible that further manipulation of the structure will result in even lower energies. We compare the original structure (a) to the (current) minimum energy LDA structure (b) in the first part of Fig. 13.

We also relaxed the original structure of Aydin using the PBE and vdW-DF2 functionals. Both quickly relaxed away from the original structure and into the results shown in Fig. 13. Note that in the vdW-DF2 structure, the system has separated into layers of WN_2 and N_2 molecules. It is unlikely that such a system could be very hard.

The minimum energy lattice constants and elastic constants for the structures shown in Fig. 13 are given in Table VIII. In the interest of saving space, we list the atomic positions in the supplementary material. While the structure labeled (a) has rather large elastic constants and so might be considered a hard material, the other

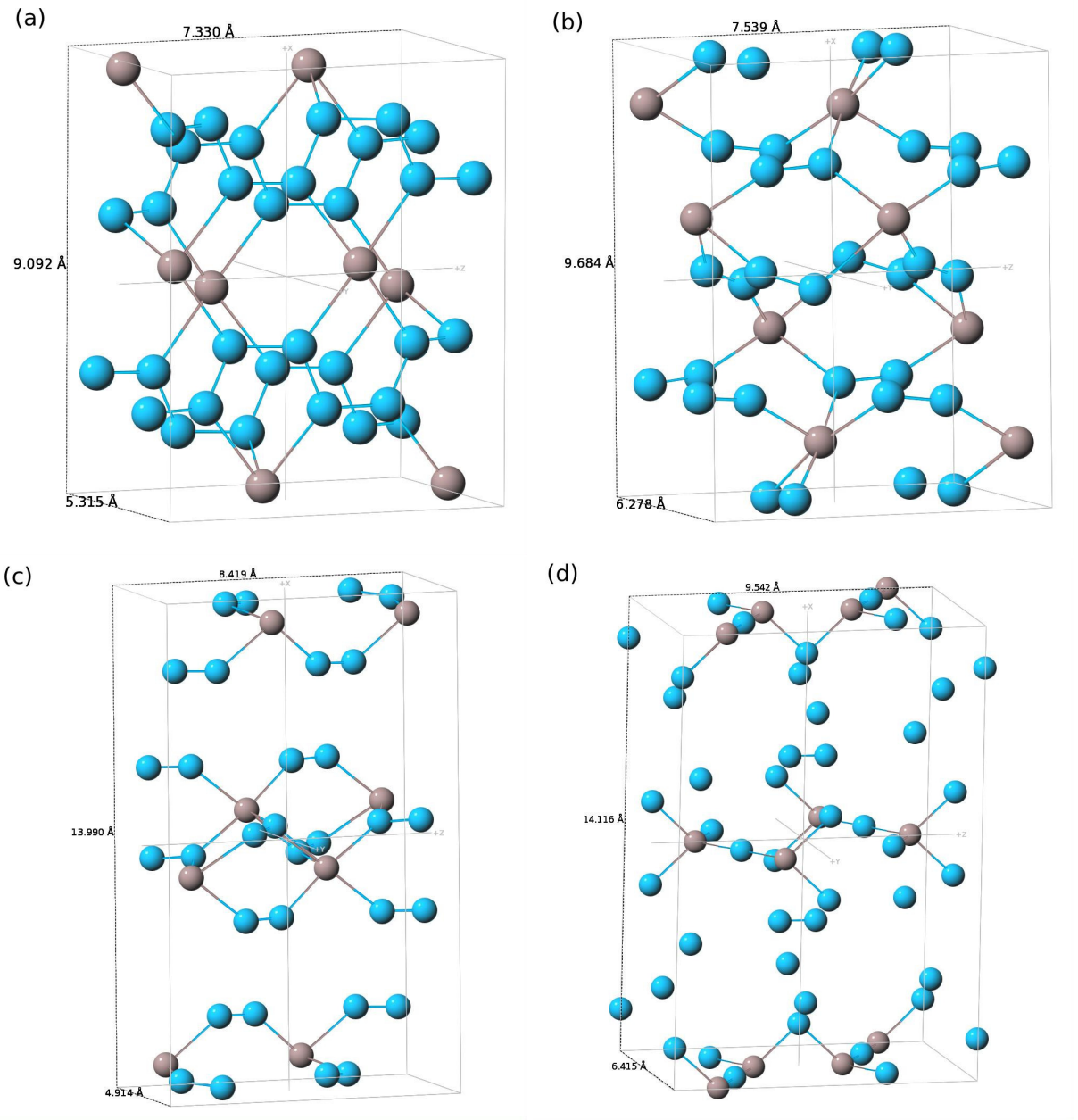


FIG. 13: Possible metastable primitive cells of N_4W in the ReP_4 structure. The distances are the values of the orthorhombic lattice constants (a, b, c) which locally minimize the total energy. The LDA functional was used for (a) and (b), which correspond the the structures referred to in Fig. 12. The minimum energy structure for the PBE functional is shown in (c), and the minimum energy structure for the vdW-DF2 functional is shown in (d). Minimum energy lattice and Wyckoff position parameters for all structures are given in the supplementary material.

structures do not. Since the (b) structure is lower in energy than the (a) structure within the LDA, we conclude that the ReP_4 structure of N_4W is not a hard material, assuming it can be made. We also note that we cannot guarantee that any of the structures studied here is the true minimum energy structure of ReP_4. There are too many possible local minima to search through at this time.

The negative elastic constants for C_{44} in the LDA (b) structure and C_{55} in the PBE and vdW-DF2 structures violate the Born criteria for elastic stability. We are performing further calculations on these systems in the hope of finding still lower energy structures. Since we have already shown that the ReP_4 state is not a viable candidate for either a hard or a stable phase in the WN system, we will defer discussion of these results.

TABLE VIII: Lattice constants and elastic constants for the WN_4 structures shown in Fig. 13. Elastic constants were computed within VASP using finite distortions of the unit cell, and include the internal relaxation of the atoms to the strain. Structure labels refer to the structures shown in Fig. 13. Lattice constants are in Ångströms, while elastic constants are in GPa.

Structure	(a)	(b)	(c)	(d)
Functional	LDA	LDA	PBE	vdW-DF2
a	9.093	9.662	13.273	14.116
b	5.314	6.279	4.927	6.415
c	7.330	7.532	8.402	9.542
C_{11}	742.1	86.8	12.1	14.6
C_{22}	159.2	96.6	138.9	131.3
C_{33}	660.1	232.6	279.7	132.8
C_{44}	23.7	-11.9	55.5	20.5
C_{55}	383.0	7.5	-3.2	-4.7
C_{66}	74.4	87.8	2.8	1.0
C_{12}	102.5	42.3	4.6	5.5
C_{13}	314.6	58.8	8.0	2.9
C_{23}	47.3	82.4	69.4	92.0

DISCUSSION

Modern first-principles electronic structure methods make it relatively simple to determine the minimum energy configuration, band structure, and total energy for any reasonably sized structure. Once that is known, it is straightforward (although frequently tedious) to determine if the structure is stable against strains and vibrations, and thus a candidate for a stable or metastable structure.

It is considerably harder to determine where a structure fits energetically compared to other structures of similar composition. In particular, we cannot determine if a given structure is stable with respect to phase separation or a structural phase transition until we determine the shape of the convex hull on the enthalpy versus composition diagram. High-throughput methods such as AFLOW make it simple to determine this hull. This approach can expediently flag low-energy structures which might be candidates for metastable states, as well as states which might be found via a pressure or temperature driven phase transition.

This paper presents a high-throughput study of the tungsten-nitrogen system. Although there have been many first-principles calculations for this system,[8–11, 19, 20] there has never before been a study of possible structures with multiple compositions. The high-throughput calculations were done using AFLOW, which we enhanced by adding known nitride, oxide, and boride structures which had not previously been included in the database. These calculations confirmed the experimental observations that tungsten nitride forms a cubic system based on the rock salt structure with vacancies (βWN).[14–17]

In fact, we found that the NbO structure (Fig. 2) is the best candidate for the ground state structure, while other states with varying patterns of vacancies produce structures nearly degenerate with NbO-WN. Most attempts to form WN compounds used high temperatures. It is thus likely that the experimental structure of WN will be the NaCl structure with approximately 25% random vacancies on both the tungsten and nitrogen sites, with some local ordering of the vacancies. This is not quite in agreement with previous experiments, where it appears that the βWN has vacancies only on the nitrogen site.[14–17] The experimental literature on the WN system is sparse, and more data is needed to confirm.

Establishing the WN convex hull allows us to evaluate the likelihood of finding other predicted forms of W_xN_{1-x}. We find that the P_3Tc structure predicted by Song and Wang,[10] as well as the ReP_4 structure predicted by Aydin *et al.*, are both well above the convex hull and thus unlikely to form, at least without special non-equilibrium processing. We did find that the hexagonal WN_2 structures predicted by Wang *et al.*[9] are stable, and of comparable enthalpy to the NbO phase – at least for calculations using the generalized-gradient PBE functional and the LDA functional.

The problem of determining the convex hull in WN is exacerbated by the fact that the ground state and other low-energy structures of N_2 are van der Waals solids. As shown in Table I, neither the LDA nor the PBE functionals adequately describe the ground state αN_2. Both correctly describe the bond length of the N-N dimer, but LDA substantially underestimates the equilibrium lattice constant while PBE drastically overestimates it. Since molecular nitrogen is van der Waals bound, we also looked at the system using the vdW-DF2 functional proposed by Dion *et al.*[32], which is readily implementable in VASP.[43, 44] This produces a much better, although still imperfect, lattice constant for αN_2.

While it is not entirely clear that the vdW-DF2 functional can be used to study dense bulk systems, we have applied it to this system across all compositions. As seen in Fig. 5, this produces little change on the tungsten-rich side of the phase diagram, but a dramatic change on the nitrogen-rich side. The vdW-DF2 functional favors the cubic cI36 structure (Fig. 10 and Table VI for WN_2, making it competitive in enthalpy/atom with the NbO structure. The hexagonal WN_2 structures, which are the ground state structures in the LDA and PBE, move up significantly. This is consistent with the limited amount of experimental data we have: no bulk hexagonal WN_2 phase has been seen. Meanwhile the ground state NaCl-like structures, with vacancies, have been seen experimentally.

Much work remains to be done on this system. We have essentially ignored the hexagonal δ phases,[16]

which are seen experimentally in thin films. This requires yet another exhausting search for vacancy patterns in supercells, this time starting from hexagonal and rhombohedral unit cells. Given the relatively low energy position of the δ_H^I phase, especially in the LDA calculation, a proper study of vacancy positions is likely to change the right-hand side of the convex hull.

We also need to study the effects of pressure. Does the application of pressure appreciably change the phase diagram, especially on the right-hand side? Given the extremely open nature of the cI36 structure, even modest pressure may trigger a first-order phase transition to another structure. We also need to perform more calculations to establish the validity of the vdW-DF2 functional when used in bulk systems. We will pursue these calculations in the future.

In conclusion, we have used high-throughput density functional calculations to study the tungsten-nitrogen phase diagram, both with and without van der Waals forces. Our calculations agree with experiment in that the dominant structure of W-N is the NaCl structure with vacancies, and show that this structure can persist over a large range of compositions. It is unlikely that many of the previously predicted nitrogen-rich phases will ever be seen experimentally, as they are well above the ground state hull. The only exceptions may be the hexagonal WN_2 phases predicted by Wang *et al.*[9] These are on the ground state hull when we use the LDA and PBE functionals, but not when we include van der Waals forces. In addition, the bulk and shear moduli of the predicted cubic ground state has rather large bulk and shear moduli, comparable with any of the previously predicted ultra-incompressible structures.[9–11]

ACKNOWLEDGMENTS

Most computational work was done at the US Naval Academy and at the ERDC and AFRL High Performance Computer Centers of the U.S. Department of Defense. We thank Fulton Supercomputing Laboratory and the Cray Corporation for additional computational support. M.J.M. is supported by the Office of Naval Research. D.F. was supported by the Naval Research Laboratory-U.S. Naval Academy Cooperative Program for Scientific Interchange. C.D. was supported by the "Simulation of Materials Under Pressure" Internship at the Naval Research Laboratory. S.C. acknowledges support from DOD-ONR (Grants No. N00014-13-1-0635, No. N00014-11-1 0136, and No. N00014-09-1-0921). G.L.W.H. is grateful for support from the National Science Foundation, Grant No.DMR-0908753. The authors thank Y. Ciftci for providing us with the starting coordinates for the ReP_4 structure used in Ref. 11, and also thank Dr. Ohad Levy and Dr. Allison Stelling for useful comments.

* michael.mehl@nrl.navy.mil
† stefano@duke.edu

[1] R. B. Kaner, J. J. Gilman, and S. H. Tolbert, *Science*, Designing Superhard Materials **308**, 1268–1269 (2005).
[2] F. J. Ribeiro, P. Tangney, S. G. Louie, and M. L. Cohen, *Hypothetical hard structures of carbon with cubic symmetry*, Phys. Rev. B **74**, 172101 (2006).
[3] A. O. Lyakhov and A. R. Oganov, *Evolutionary search for superhard materials: Methodology and applications to forms of carbon and TiO_2*, Phys. Rev. B **84**, 092103 (2011).
[4] T. E. Mosuang and J. E. Lowther, *Relative stability of cubic and different hexagonal forms of boron nitride*, J. Phys. Chem. Solids **63**, 363–368 (2002).
[5] S. Vepřek, *The search for novel, superhard materials*, J. Vac. Soc. Technol. A **17**, 2401–2420 (1999).
[6] A. Ivanovskii, *Mechanical and electronic properties of diborides of transition 3d-5d metals from first principles: Toward search of novel ultra-incompressible and superhard materials*, Prog. Mat. Sci. **57**, 184–228 (2012).
[7] X. Hao, Y. Xu, Z. Wu, D. Zhou, X. Liu, X. Cao, and J. Meng, *Low-compressibility and hard materials ReB_2 and WB_2: Prediction from first-principles study*, Phys. Rev. B **74**, 224112 (2006).
[8] D. V. Suetin, I. R. Shein, and A. L. Ivanoskii, *Elastic and electronic properties of hexagonal and cubic polymorphs of tungsten monocarbide WC and mononitride WN from first-principles calculations*, Phys. Stat. Sol. B **245**, 1590–1597 (2008).
[9] H. Wang, Q. Li, Y. Li, Y. Xu, T. Cui, A. R. Oganov, and Y. Ma, *Ultra-incompressible phases of tungsten dinitride predicted from first principles*, Phys. Rev. B **79**, 132109 (2009).
[10] L. Song and Y.-X. Wang, *First-principles study of W, WN, WN_2, and WN_3*, Phys. Stat. Sol. B **247**, 54–58 (2010).
[11] S. Aydina, Y. O. Ciftci, and A. Tatar, *Superhard transition metal tetranitrides: XN_4 (X = Re, Os, W)*, J. Mater. Res. **27**, 1705–1715 (2012).
[12] J. Donohue, *The Structures of the Elements* (John Wiley & Sons, New York, 1974).
[13] H. A. Wriedt, *The N-W (Nitrogen-Tungsten System*, Bulletin of Alloy Phase Diagrams **10**, 358–367 (1989).
[14] G. Hägg, *X-ray Diffraction Investigations on Molybdenum and Tungsten Nitrides*, Z. Phys. Chem. B **7**, 339–362 (1930).
[15] V. I. Khitrova and Z. G. Pinsker, *An electron-diffraction study of cubic tungsten nitride*, Sov. Phys. Crystallogr. **4**, 513–520 (1959).
[16] V. I. Khitrova and Z. G. Pinsker, *Chemical Crystallography of Tungsten Nitrides and of Some Other Interesting Phases*, Sov. Phys. Crystallogr. **6**, 712–719 (1962).
[17] V. I. Khitrova, *WN_2 Structure*, Sov. Phys. Crystallogr. **6**, 439–442 (1962).
[18] N. Schönberg, *Contributions to the Knowledge of the Molybdenum-Nitrogen and the Tungsten-Nitrogen Systems*, Acta Chem. Scan. **8**, 204–207 (1954).
[19] E. I. Isaev, S. I. Simak, I. A. Abrikosov, R. Ahuja, Y. K. Vekilov, M. I. Katsnelson, A. I. Lichtenstein, and B. Johansson, *Phonon related properties of transition metals, their carbides, and nitrides: A first-principles study*,

J. Appl. Phys. **101**, 123519 (2007).

[20] P. Kroll, T. Schröter, and M. Peters, *Prediction of Novel Phases of Tantalum(V) Nitride and Tungsten(VI) Nitride That Can Be Synthesized under High Pressure and High Temperature*, Angew. Chem. Int. Ed. **44**, 4249–4254 (2005).

[21] S. Curtarolo, W. Setyawan, G. L. W. Hart, M. Jahnatek, R. V. Chepulskii, R. H. Taylor, S. Wang, J. Xue, K. Yang, O. Levy, M. Mehl, H. T. Stokes, D. O. Demchenko, and D. Morgan, *AFLOW: an automatic framework for high-throughput materials discovery*, Comp. Mat. Sci. **58**, 218–226 (2012).

[22] S. Curtarolo, G. L. W. Hart, M. Buongiorno Nardelli, N. Mingo, S. Sanvito, and O. Levy, *The high-throughput highway to computational materials design*, Nature Mater. **12**, 191–201 (2013).

[23] O. Levy, G. L. W. Hart, and S. Curtarolo, *Structure maps for hcp metals from first-principles calculations*, Phys. Rev. B **81**, 174106 (2010).

[24] O. Levy, M. Jahnatek, R. V. Chepulskii, G. L. W. Hart, and S. Curtarolo, *Ordered Structures in Rhenium Binary Alloys from First-Principles Calculations*, J. Am. Chem. Soc. **133**, 158–163 (2011).

[25] M. Jahnatek, O. Levy, G. L. W. Hart, L. J. Nelson, R. V. Chepulskii, J. Xue, and S. Curtarolo, *Ordered Structures and Vibrational Stabilization in Ruthenium Alloys from First Principles Calculations*, Phys. Rev. B **84**, 214110 (2011).

[26] O. Levy, J. Xue, S. Wang, G. L. W. Hart, and S. Curtarolo, *Uncovering Technetium binary ordered structures from first principles*, Phys. Rev. B **85**, 012201 (2012).

[27] *Comprehensive Search for New Phases and Compounds in Binary Alloy Systems Based on Platinum-Group Metals, Using a Computational First-Principles Approach*, Phys. Rev. X **3**, 041035 (2013).

[28] S. Curtarolo, W. Setyawan, S. Wang, J. Xue, K. Yang, R. H. Taylor, L. J. Nelson, G. L. W. Hart, S. Sanvito, M. Buongiorno Nardelli, N. Mingo, and O. Levy, *AFLOWLIB.ORG: A distributed materials properties repository from high-throughput ab initio calculations*, Comp. Mat. Sci. **58**, 227–235 (2012).

[29] J. P. Perdew, K. Burke, and M. Ernzerhof, *Generalized Gradient Approximation Made Simple*, Phys. Rev. Lett. **77**, 3865–3868 (1996).

[30] D. M. Ceperley and B. J. Alder, *Ground State of the Electron Gas by a Stochastic Method*, Phys. Rev. Lett. **45**, 566–569 (1980).

[31] J. P. Perdew and A. Zunger, *Self-interaction correction to density-functional approximations for many-electron systems*, Phys. Rev. B **23**, 5048–5079 (1981).

[32] M. Dion, H. Rydberg, E. Schroder, D. C. Langreth, and B. I. Lundqvist, *Van der Waals Density Functional for General Geometries*, Phys. Rev. Lett. **92**, 246401 (2004).

[33] S. Curtarolo, G. L. W. Hart, W. Setyawan, M. J. Mehl, M. Jahnatek, R. V. Chepulskii, O. Levy, and D. Morgan, *AFLOW* (2010). Software for High-Throughput Calculation of Material Properties.

[34] G. Kresse and J. Hafner, Ab initio *molecular dynamics for open-shell transition metals*, Phys. Rev. B **48**, 13115–13118 (1993).

[35] G. Kresse and J. Hafner, Ab initio *molecular-dynamics simulation of the liquid-metal/amorphous-semiconductor transition in germanium*, Phys. Rev. B **49**, 14251–14269 (1994).

[36] G. Kresse, , Ph.D. thesis, Technische Universität Wien, Vienna (1993).

[37] G. Kresse and D. Joubert, *From ultrasoft pseudopotentials to the projector augmented-wave method*, Phys. Rev. B **59**, 1758–1775 (1999).

[38] P. E. Blöchl, *Projector augmented-wave method*, Phys. Rev. B **50**, 17953–17979 (1994).

[39] K. Dewhurst, S. Sharma, L. Nordström, F. Cricchio, F. Bultmark, H. Gross, C. Ambrosch-Draxl, C. Persson, C. Brouder, R. Armiento, A. Chizmeshya, P. Anderson, I. Nekrasov, F. Wagner, F. Kalarasse, J. Spitaler, S. Pittalis, N. Lathiotakis, T. Burnus, S. Sagmeister, C. Meisenbichler, S. Lebégue, Y. Zhang, F. Körmann, A. Baranov, A. Kozhevnikov, S. Suehara, F. Essenberger, A. Sanna, T. McQueen, T. Baldsiefen, M. Blaber, A. Filanovich, T. Björkman, M. Stankovski, J. Goraus, M. Meinert, D. Rohr, V. Nazarov, K. Krieger, A. Davydov, F. Eich, and A. R. Castro, *ELK*. The ELK Full-potential LAPW code.

[40] P. Hohenberg and W. Kohn, *Inhomogeneous Electron Gas*, Phys. Rev. **136**, B864–B871 (1964).

[41] W. Kohn and L. J. Sham, *Self-Consistent Equations Including Exchange and Correlation Effects*, Phys. Rev. **140**, A1133–A1138 (1965).

[42] M. I. Eremets, R. J. Hemley, H. kwang Mao, and E. Gregoryanz, *Semiconducting non-molecular nitrogen up to 240 GPa and its low-pressure stability*, Naturere **411**, 170–174 (2001).

[43] J. Klimeš, D. R. Bowler, and A. Michaelides, *Chemical accuracy for the van der Waals density functional*, J. Phys.: Condens. Matt. **22**, 022201 (2010).

[44] J. Klimeš, D. R. Bowler, and A. Michaelides, *Van der Waals density functionals applied to solids*, Phys. Rev. B **83**, 195131 (2011).

[45] H. J. Monkhorst and J. D. Pack, *Special points for Brillouin-zone integrations*, Phys. Rev. B **13**, 5188–5192 (1976).

[46] MedeA, Materials Design Inc.

[47] M. J. Mehl, J. E. Osburn, D. A. Papaconstantopoulos, and B. M. Klein, *Structural properties of ordered high-melting-temperature intermetallic alloys from first-principles total-energy calculations*, Phys. Rev. B **41**, 10311–10323 (1990). *erratum* Phys. Rev. B **42**, 5362 (1990).

[48] M. J. Mehl, B. M. Klein, and D. A. Papaconstantopoulos, *First-Principles Calculation of Elastic Properties*, in *Intermetallic Compounds - Principles and Practice*, edited by J. H. Westbrook and R. L. Fleischer (John Wiley and Sons, London, 1995), vol. 1, chap. 9, pp. 195–210.

[49] C. Kittel, *Introduction to Solid State Physics* (John Wiley & Sons, New York, 1996), 7^{th} edn.

[50] F. Birch, *Finite strain isotherm and velocities for single-crystal and polycrystalline nacl at high-pressures and 300-degree-k*, J. Geophys. Res. **83**, 1257–1268 (1978).

[51] G. Simmons and H. Wang, *Single Crystal Elastic Constants and Calculated Aggregate Properties: A HANDBOOK* (M.I.T. Press, Cambridge, Massachusetts and London, 1971), 2^{nd} edn.

[52] C. M. L. H. Yang and A. K. McMahan, *Polymeric nitrogen*, Phys. Rev. B **46**, 14419–14435 (1992).

[53] J. P. Perdew, J. A. Chevary, S. H. Vosko, K. A. Jackson, M. R. Pederson, D. J. Singh, and C. Fiolhais, *Atoms, molecules, solids, and surfaces: Applications of the generalized gradient approximation for exchange and corre-*

lation, Phys. Rev. B **46**, 6671–6687 (1992).

[54] H.-T. Chiu and S.-H. Chuang, *Tungsten nitride thin films prepared by MOCVD*, J. Mater. Res. **8**, 1353–1360 (1993).

[55] M. Born, Proc. Cambridge Philos. Soc. **36**, 160 (1940).

[56] Z. Hashin and S. Strikman, *On some variational principles in anisotropic and nonhomogeneous elasticity*, J. Mech. Phys. Solids **10**, 335–342 (1962).

[57] Z. Hashin and S. Shtrikman, *A variational approach to the theory of the elastic behaviour of polycrystals*, J. Mech. Phys. Solids **10**, 343–352 (1962).

[58] M. Zumbusch, *Über die Strukturen des Uransubsulfids und der Subphosphide des Iridiums und Rhodiums*, Z. Anorg. Allg. Chem. **243**, 322–329 (1940).

[59] T.-S. Chang and P. Trucano, *Lattice parameter and thermal expansion of ReO_3 between 291 and 464 K*, J. Appl. Cryst. **11**, 286–288 (1978).

[60] W. Voigt, *Lehrbuch der Kristallphysik* (Teubner, Leipzig, 1928).

[61] A. Reuss, *Berechnung der Fließgrenze von Mischkristallen auf Grund der Plastizitätsbedingung für Einkristalle*, Z. Angew. Math. Mech. **9**, 49–58 (1929).

[62] T. Siegrist and F. Hulliger, *High-temperature behavior of $CoAs_2$ and $CoSb_2$*, J. of Solid St. Chem. **63**, 23–30 (1896).

[63] D. A. Evans and K. H. Jack, *The $\gamma \rightarrow \beta$ phase transformation in the Mo-N system*, Acta Cryst. **10**, 833–834 (1957).

[64] U. C. Rodewald, R.-D. Hoffman, Z. Wu, and R. Pöttgen, *Structure Refinement of $AuSN_2$*, Z. Naturerforsch. **61**, 108–110 (2006).

[65] R. Rühl and W. Jeitschko, *Preparation and structure of technetium triphosphide and rhenium triphosphide, isotypic polyphosphides with metal chains*, Acta Cryst. B **38**, 2784–2788 (1982).

[66] G. Andersson and A. Magnéli, *On the Crystal Structure of Molybdenum Trioxide*, Acta Chem. Scan. **4**, 793–797 (1950).

[67] W. Jeitschko and R. Rühl, *Synthesis and crystal structure of diamagnetic ReP_4, a polyphosphide with Re-Re pairs*, Acta Cryst. B **35**, 1953–1958 (1979).